A Comparison of the Decomposition of Biomass Gasification Tar compound in CO, CO_2, H_2 and N_2 carrier gases using Non-thermal plasma

Faisal Saleem[1, 2*], Abdul Rehman[1], Aumber Abbas[1], Asif Hussain khoja[3], Farhan Ahmad[4], Lina Liu[4], Kui Zhang[1], Adam Harvey[1]

[1]School of Engineering, Newcastle University Newcastle upon Tyne NE1 7RU

[2]Department of Chemical and Polymer Engineering, University of Engineering and Technology, Lahore, Faisalabad Campus, Pakistan

[3]Department of thermal energy engineering, National university of science and technology, Islamabad, Pakistan

[4]Department of chemical engineering, University of Engineering and Technology, Lahore, Pakistan

[5]MOE Key Laboratory of Pollution Processes and Environmental Criteria, College of Environmental Science and Engineering, Nankai University, 38 Tongyan Road, Jinnan District, Tianjin 300350, China

Abstract

In this study, a comparative decomposition of toluene was investigated using a dielectric barrier discharge (DBD) reactor. The first-time decomposition of the tar model compound was investigated in pure CO gas. The effect of each carrier gas (N_2, H_2, CO_2 and CO), which exists in product gas from the gasifier, was studied on the decomposition of tar analogue (toluene) and product distribution. The specific input energy (SIE) was also varied from 2.5–8.5 kJ/L to investigate the optimal removal of tar analogue. The maximum removal of toluene was 89.1 % using N_2 as carrier gas at 8.5 kJ/L and 1.43 s. However, the minimum removal of toluene was 62.5% using CO carrier gas under the same conditions. The decomposition of toluene in

different carrier gases was in the following order: CO < CO_2 < H_2 < N_2. Moreover, the distribution of products depends on the nature of the carrier gas as well. However, lower hydrocarbons (LHC) (< C_7) and solid residues were observed in each carrier gas. The maximum yield of LHC was about 10.8% in H_2 carrier gas, whereas in CO and CO_2 it remained below 1% even at 8.5 kJ/L.

Keywords: Tar removal, Dielectric barrier discharge, Biomass gasification, Non-thermal plasma

1. Introduction

The use of waste biomass as a renewable source to produce valuable products is highly desirable. This will not only help to make various supply chains 'greener' but also used as a means of reducing global warming. Biomass can be converted into synthesis gas by gasification, which converts solid biomass to gaseous fuels [1, 2]. These gaseous fuels can be used as an alternative to fossil fuels in transport and power generation sectors [3]. Also, it can be used for the production of liquid fuels, hydrogen, and many other useful chemicals [4-6]. The product gas composition depends on various parameters, such as gasifying medium (air, steam, or oxygen), operating conditions, gasification methods, nature of feedstock, etc. The product gas typically comprises CO_2, H_2, N_2, CO and various LHC when air is used as a gasification medium [1]. Additionally, impurities like ash, particulates, tars and volatile alkali metals are also produced [1, 7, 8]. Among these impurities, tar compounds create various technical challenges as it may condense in the heat exchangers, connecting pipes, filters and engines, reducing heat transfer and ultimately causing blockages. Subsequently, the process efficiency decreases and the maintenance cost increases [9-12]. Therefore, tar removal is highly desirable for the successful operation of biomass gasification on a commercial scale.

Recently, non-thermal plasma (NTP) was considered as an attractive alternative for gasifier product gas cleaning technologies due to its ability to considerably raise the electrons' temperature, i.e. up to 10^4 –10^5 K [13, 14]. Among NTP reactors, dielectric barrier discharge (DBD) reactors are commonly used to treat tar compounds, volatile organic compounds (VOCs) and toxic compounds [15-27]. These studies suggest that a DBD reactor can effectively remove most of the aromatic and non-aromatic compounds present in tar. The removal of toluene as a tar analogue was also studied in a different gas environment using the DBD reactor. It was observed that the maximum removal was obtained in N_2 carrier gas in the absence of any packing materials. However, the conversion decreases when H_2, CO or CO_2 were added into N_2 [28]. It was observed that the removal of tar compounds increased with surface energy density (SED) in the DBD reactor [29]. The amount of long-chain aliphatic hydrocarbons and aromatic compounds decreases during discharge, whereas the formation of gaseous hydrocarbons enhanced. Hence, the DBD reactor has been extensively used to decompose biomass tar compounds under different operating conditions, and it is proven that it certainly helps in removing the tar model compounds.

In this study, toluene was chosen as a model 'Tar' compound due to its presence in abundance in large quantities during the high-temperature biomass gasification [30]. Moreover, the low boiling point and high thermal stability of toluene make it an excellent choice to use as a tar analogue [31]. Furthermore, the simple aromatic structure of toluene also helps to perform mechanistic investigation during tar cracking using NTP at ambient conditions. Previous studies of toluene decomposition as a tar analogue were mostly investigated using N_2 as a carrier gas [31-35]. The addition of CO_2 and H_2O in nitrogen carrier gas was also investigated to study the conversion of toluene, energy efficiency, and gas production. It was observed that the addition of CO_2 decreases the decomposition of toluene, whereas the maximum decomposition of toluene obtained at 16% steam. However, both additives decreased carbon

deposition, and syngas was the major product [36]. It was reported that the optimum amount of steam reduced carbon black and improved H_2 yield and facilitate tar conversion. However, a higher concentration reduced the decomposition of tar compounds [37]. A similar effect of steam was reported using microwave plasma. It was reported that increasing the addition of steam increasing the decomposition of tar compound and promoted the formation of CO, CO_2, and H_2 [38]. To study the effect of carrier gas, a comparative study of benzene decomposition as a tar analogue was also carried out in a DBD reactor using CO_2 and H_2 as carrier gases [39]. This study showed that a higher decomposition of benzene using H_2 as a carrier gas due to lower bond-dissociation energy of H_2 which can generate reactive H radicals.

The product gas from a biomass gasifier mainly consists of CO_2, H_2, CO, and N_2. Therefore, in this study, the decomposition of toluene as a tar surrogate was investigated using CO_2, H_2, CO, and N_2 as carrier gases to understand the contribution of each gas. As per our knowledge, the comparative role of major components of fuel gas is not investigated for the removal of tar compound using DBD reactor. The decomposition of tar compounds in pure CO carrier gas is also investigated due to the presence of it in the gasifier product gas, which is not present in any literature until now. Therefore, a comparative analysis of toluene decomposition could be helpful for a better understanding of the NTP assisted tar removal. These observations are essential for the development of a novel technique used for tar removal from the product gas with high energy efficiency at low temperatures and ambient pressure.

2. Experimental setup

The schematic figure of the experimental setup is shown in figure 1. The non-thermal plasma DBD reactor was used to study the decomposition of tar compound. Stainless steel (SS) external electrode (45 mm) was wrapped outside the external quartz tube which has 15 mm

internal diameter. The inner SS electrode was put inside the internal quartz tube with an outer diameter of 12 mm.

A variac AC transformer was connected to the plasma generator to regulate the discharge power to the DBD reactor. In current study, the input power was varied from 5 to 17 W. The supplied power was measured using the energy meter. The discharge zone depends on the external electrode (shortest electrode). The flow rate of each carrier gas was fixed at 120 ml/min using computer-controlled mass flow controllers to control the flow rate of different gases. The composition of different products was measured by a Varian 450-GC equipped with a flame ionization detector (FID) and thermal conductivity detector (TCD).

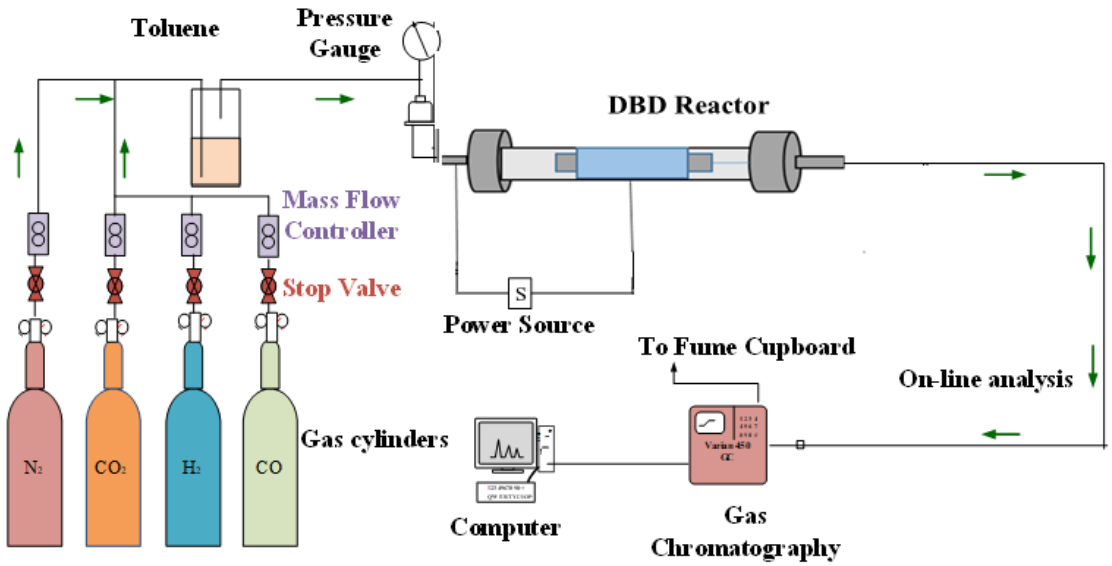

Fig. 1 Schematic figure of the experimental setup

2.1 Definitions

The toluene decomposition is defined as follows:

$$d_T = \frac{\text{amount of toluene in - amount of toluene out}}{\text{amount of toluene in}} \times 100$$

The following formulae were used to calculate the yield of different products:

$$\text{LHC yield (\%)} = \frac{\sum (m \times \text{moles of} C_mH_n)}{7 \times \text{Moles of } C_7H_8 \text{ input}} \times 100$$

$$H_2 \text{ yield (\%)} = \frac{\text{moles of } H_2 \text{ produced}}{4 \times \text{ Moles of } C_7H_8 \text{ input}} \times 100$$

$$\text{CO yield (\%)} = \frac{\text{total moles of CO in the outlet stream}}{(7 \times C_7H_8 \text{ moles input}) + CO2 \text{ moles input}} \times 100$$

The yield of products was calculated based on total carbon/hydrogen input.

$$\text{Specific input energy (SIE)} \left(\frac{\text{kJ}}{\text{L}}\right) = \frac{\text{P (W)} \times 60}{1000 \times \text{Flow rate total (L/min)}}$$

The energy efficiency was calculated as follows:

$$\text{Energy efficiency (EE)} \left(\frac{\text{g}}{\text{kWh}}\right) = \frac{\text{amount of toluene decomposed (g/min)} \times 60000}{\text{P (W)}}$$

3. Results and Discussion

3.1 Decomposition of tar compound

Fig. 2 indicates the effect of different carrier gases on the conversion of toluene at various levels of SIE. The conversion of toluene increases with the increase in SIE. At higher values of SIE more power was supplied to the reactor, since SIE was varied by changing input power at a constant flow rate. It was reported that an increase in the power could increase the electron density and gas temperature [40]. Therefore, a higher conversion is likely to be achieved due to the presence of a high number of energetic electrons. The significant role of energetic electrons in toluene decomposition was also reported elsewhere [18].

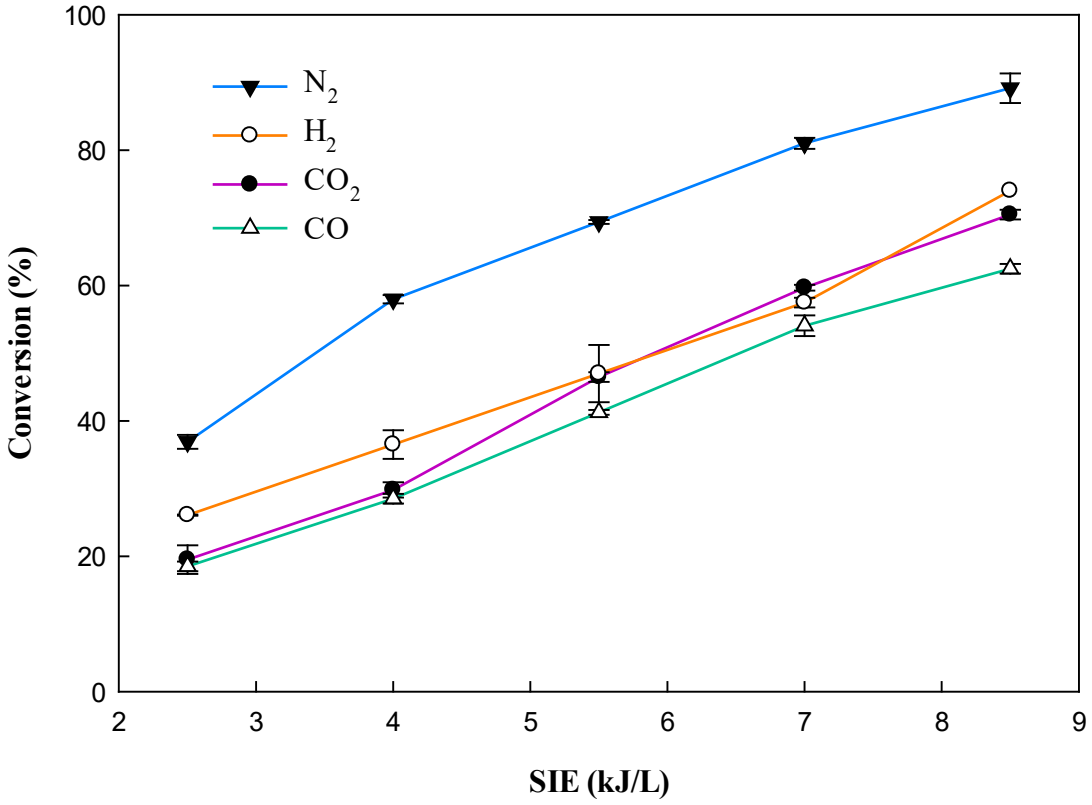

Fig. 2. Effect of carrier gas and SIE on the conversion of toluene. Reaction conditions: power, 5–17 W; concentration, 33 g/Nm^3; flow rate, 120 ml/min; and residence time, 1.43 s.

Moreover, these energetic electrons interact with background gas molecules to produce ions, radicals and other electronically excited species. These highly reactive species can also contribute to the conversion of the tar model compound. Fig. 2 also shows that the conversion of toluene increases in the following order; CO < CO_2 < H_2 < N_2. The maximum conversion was obtained in the presence of N_2 carrier gas.

In another study, it was observed that the decomposition of toluene in N_2 occurred due to energetic electrons and excited molecular states of nitrogen (N_2 ($A^3\sum_u^+$) ,N_2 ($B^3\prod_g$) and N_2 ($C^3\prod_u$)) [31, 41]. Furthermore, the reactions of N_2 ($A^3\sum_u^+$) (metastable nitrogen) with tar molecules significantly contributed in decomposition of tar molecules [42]. It was further revealed that the cracking of naphthalene started by nitrogen excited states, whereas the effect

of electrons (energetic) was not significant [43-45]. Therefore, all these factors may contribute to higher conversion of toluene in N_2 as the carrier gas. CO_2 shows less conversion than H_2 and N_2 carrier gas. In CO_2 carrier gas, the reactive species may produce through electro ionization dissociation channels and electron impact dissociation [46]. It is reported that the bond dissociation energy of the CO_2 is 5.5 eV, whereas the mean electron energy is in the range of 1-10 eV [47]. In H_2 carrier gas, the bond dissociation energy of H_2 (4.53 eV) is less than other carrier gases. Therefore, the presence of H radicals in H_2 carrier gas gave higher conversion than CO_2 and CO Carrier gas.

3.2 Energy efficiency

Fig. 3 shows the energy efficiency of the process. It can be observed that energy efficiency decreases in N_2 and H_2 carrier gases with increasing SIE. It is reported that the energy efficiency of the plasma processes decreases due to diminishing returns [48]. However, there is no significant change observed in energy efficiency in CO and CO_2 carrier gases. In the current set of experiments, the energy efficiency depends on the decomposition of toluene, and power, whereas all other parameters (concentration of toluene and flow rate) were kept constant. The decomposition of toluene also varies with power. Increasing power directly increases the decomposition of toluene, which increases the total amount of decomposed toluene. In a nutshell, the energy efficiency based on the total amount of decomposed toluene with respect to power. If it increases directly with increasing power, then energy efficiency will also show the same. However, in the presence of N_2 carrier gas with increasing power from 5 to 17 W (>3 times), the conversion only increases from 36.5 to 89.1% (<3 time), which affects the amount of total decomposed toluene. Therefore, the energy efficiency decreases with increasing power. A similar trend was also observed in H_2 carrier gas due to this reason. This is consistent with previous experimental studies [31, 49, 50]. Similarly, it also decreases when the mixture of different carrier gases was used in the DBD reactor [51]. In another study, the

decomposition of toluene was studied using a rotating gliding arc discharge reactor [31]. The higher energy efficiency (16.61 g/kWh) was reported as compared to the previous study (4.52 g/kWh) where microwave plasma torch was used [52]. However, in the current study, the maximum energy efficiency was 17.5 g/kWh in N_2 carrier gas which started to decrease with increasing power.

In CO_2 carrier gas, the percentage decomposition of toluene increase from 19.5 to 70.5 (>3.5 times) % when power increases from 5 W to 17 W (<3.5 times). Therefore, the amount of decomposed toluene increases a little bit higher than power. Due to the high conversion rate of toluene, the energy efficiency of CO_2 also increases slightly. In CO carrier gases, the percentage decomposition of toluene increases from 18.5–62.5% (3.4 times) when power increases from 5–17 W (3.4 times). Due to nearly the same increase in both parameters, the energy efficiency does not increase with increasing power.

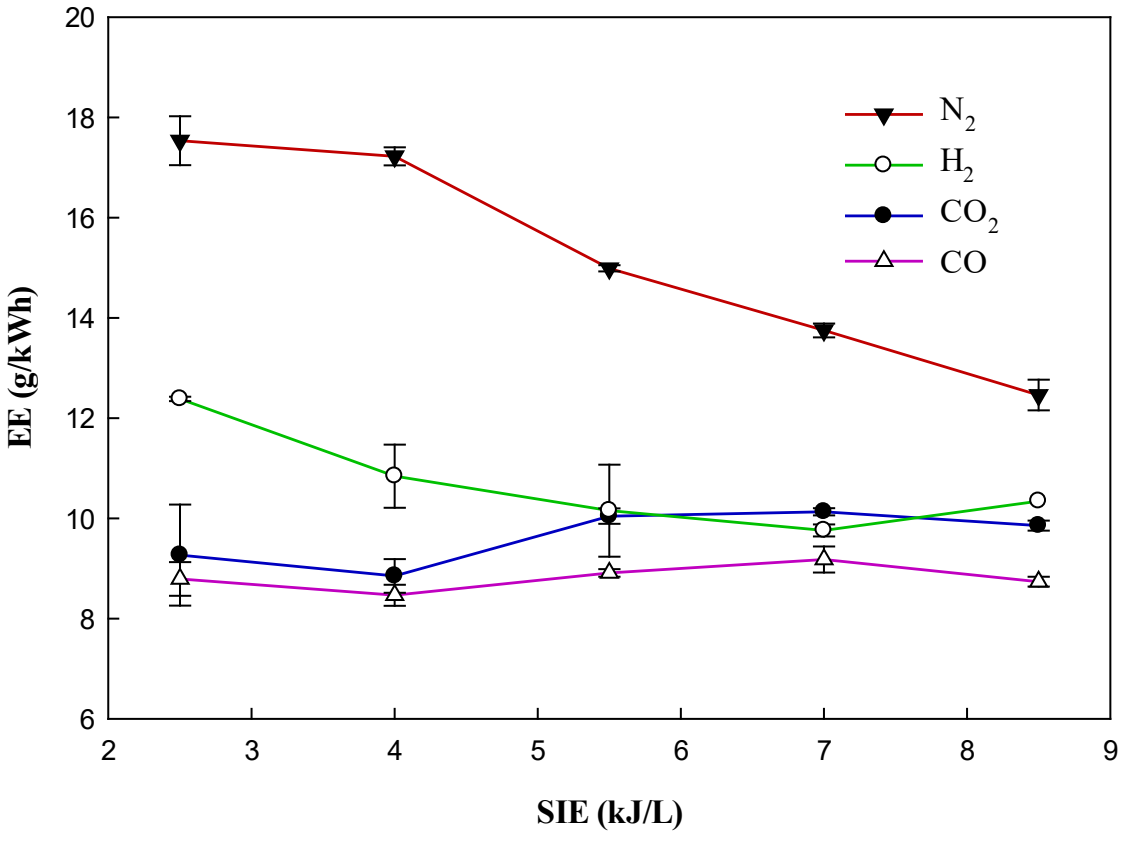

Fig. 3. Effect of carrier gas and SIE on energy efficiency. Reaction conditions: power, 5–17 W; concentration, 33 g/Nm^3; flow rate, 120 ml/min; and residence time, 1.43 s

3.3 Yield of Lower hydrocarbons (LHC)

The yield of LHC in different carrier gases has shown in Fig.4. The yield of LHC is maximum using H_2 as a carrier gas and it increases with SIE. It is reported in the literature that the thermal cracking of toluene produces methane and benzene in H_2 carrier gas at 750ºC [53]. It was suggested that hydrogen reacted with benzyl, methyl and phenyl radicals and acted as a scavenger for these radicals. However, in the current study, reactive species produce H radicals at ambient conditions, which react with intermediates to produce LHC. The formation of reactive species also increases with increasing SIE. Therefore, the yield of LHC increases with increasing SIE. It was observed that the yield of LHC was remained below 1% in CO_2 and CO carrier gases, whereas it was about 2% in N_2. The possible reason for the lower yield of LHC was the hydrogen deficit environment in CO_2, CO, and N_2. The intermediate compounds having aromatic ring can combine to produce solid residues. Therefore, a significant reduction in the amount of carbon was noted in the case of all carrier gases. Moreover, the solid residues obtained as a result of toluene decomposition were found to be black, light yellow, brown, and black/brown colour using N_2, H_2, CO, and CO_2 as carrier gases respectively. The decomposition of toluene was carried out in a non-oxidative atmosphere, which eventually increased the deposition of solid carbon [31, 35]. However, the presence of these solid residues has some drawbacks for the continuous operation of the DBD reactor. Therefore, it was required to decrease the selectivity towards solid residues using some appropriate techniques. This problem was addressed by the synergetic effect of temperature and plasma using H_2 as a carrier gas, which resulted in a significant reduction of residues formation [35, 39, 50]. The increase in selectivity to CH_4 was observed up to 60% when decomposition of toluene was carried using H_2 as carrier gas at 40 W and 400ºC [49]. Likewise, an increase in selectivity to

CH_4 was observed up to 80% when decomposition of benzene was carried under the same reaction conditions [39]. In both cases, solid residue formation completely disappeared from the reactor. The removal of solid residues also disappeared in a mixture of carrier gases at elevated temperatures in the presence of the plasma [50, 54]. Therefore, the addition of H_2 in the carrier gas can reduce unwanted by-products formation.

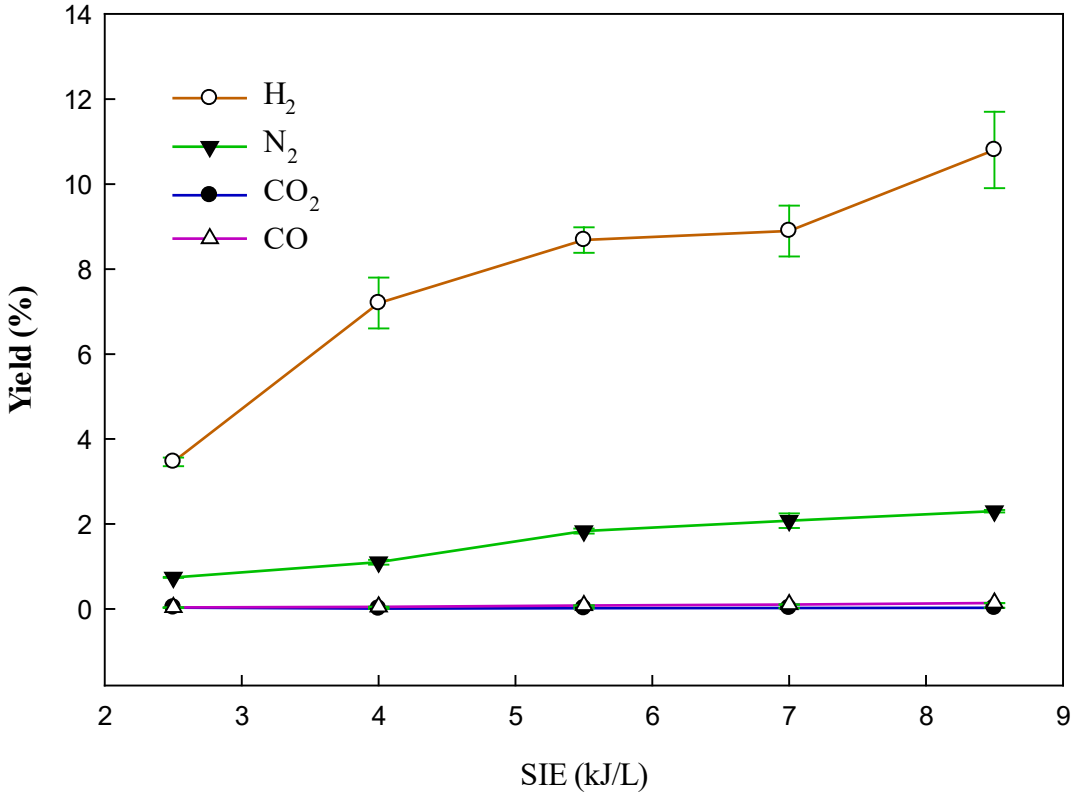

Fig. 4. Effect of carrier gas and SIE on the yield of LHC (C_1–C_6). Reaction conditions: power, 5–17 W; concentration, 33 g/Nm^3; flow rate, 120 ml/min; and residence time, 1.43 s.

3.4 Yield of CO

Fig. 5 shows the effect of SIE on the yield of CO. It can be noted that only CO_2 carrier gas produced CO due to the presence of O radicals. The major amount of CO produced through the decomposition of CO_2 [46, 48], whereas some CO may be produced through the oxidation

of toluene fragments due to the presence of O radicals. The yield of CO also increases with SIE. It is possible that due to electron impact dissociation reactions. At higher power, the density of the electrons increases which contributes towards increasing the yield of CO.

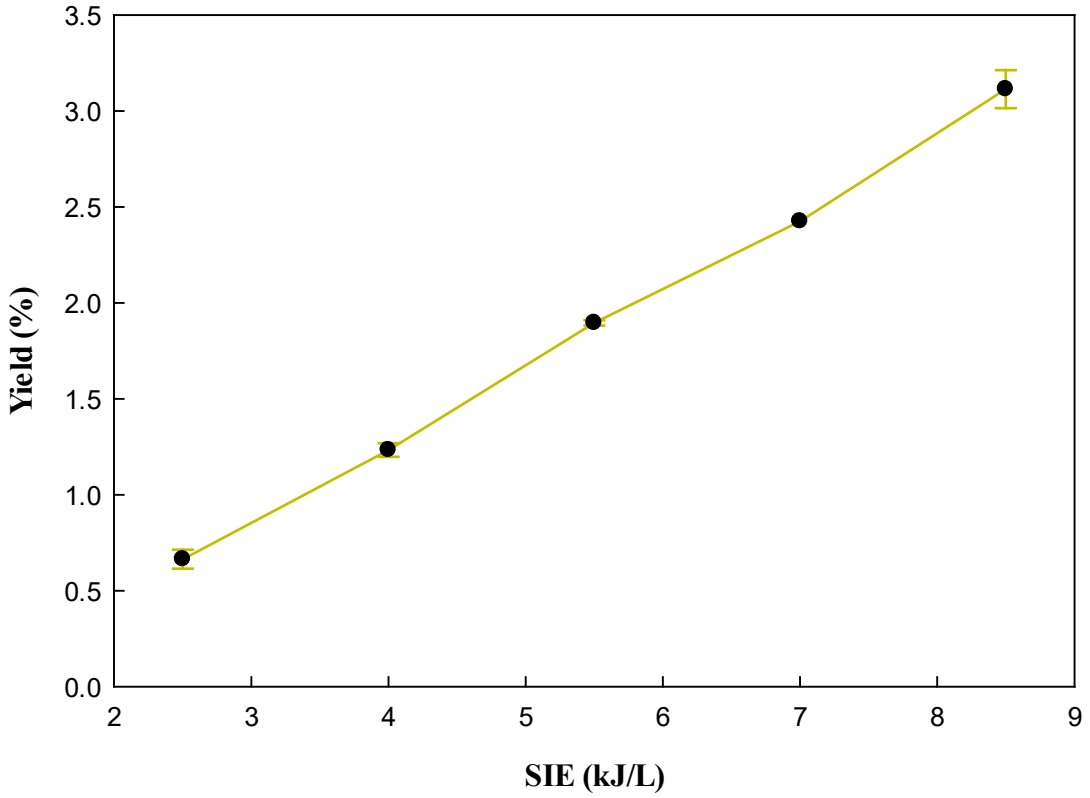

Fig. 5. Effect of SIE on the yield of CO. Reaction conditions: power, 5–17 W; concentration, 33 g/Nm^3; flow rate, 120 ml/min; and residence time, 1.43 s.

3.5 Yield of H_2

From the experimental results shown in Fig. 6, it can be seen that the yield of H_2 increases with increasing SIE. It may occur due to the presence of more reactive species at high power supplied. At lower power, reactive species abstract the H_2 from the methyl group due to its minimum bond dissociation energy in the toluene molecule [55]. However, at higher powers, due to the presence of more reactive species and energetic electrons, the yield of hydrogen increases as a result of the cleavage of the aromatic ring. The maximum yield of H_2 obtained

in N_2 Carrier gas. It was discussed above that the presence of excited states of N_2 gave a higher conversion of toluene. The reactive species may contribute higher in the production of H radicals from the abstraction of methyl as well as the aromatic ring, which can combine to produce a higher yield of H_2 as compared to CO_2, and CO carrier gases. The formation of O radicals during the decomposition of CO_2 carrier gas may also contribute to the formation of hydrogen. This may be the possible reason for the higher yield of hydrogen in CO_2 carrier gas than CO.

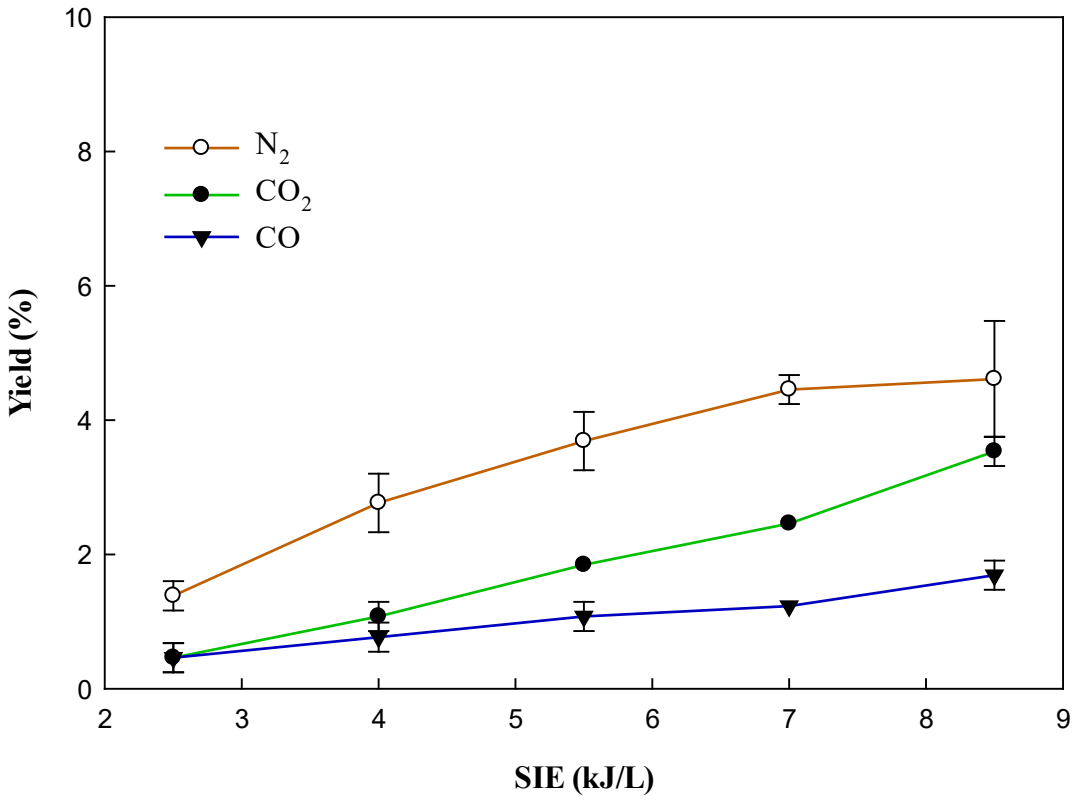

Fig. 6. Effect of carrier gas on the yield of H_2. Reaction conditions: power, 5–17 W; concentration, 33 g/Nm^3; flow rate, 120 ml/min; and residence time, 1.43 s.

246 **3.6 General Mechanism**

247 The general mechanism involved in toluene decomposition is shown in Fig.7. The toluene
248 decomposition was initiated through the H-abstraction from the methyl group, because of the
249 lowest bond dissociation energy in toluene [56]. The 2nd impact of the electron may decompose
250 the C–C bond between methyl and aromatic ring. These aromatic ring containing intermediates
251 react with each other to produce the polymer, while methane produces from the recombination
252 of CH_3 and H radicals. Simultaneously, electron and excited species may decompose the
253 aromatic ring followed by the production of LHC (< C7). In CO_2 carrier gas, the Decomposition
254 of CO_2 produces CO and O. Therefore, the presence of O also contributes to the decomposition
255 of toluene. The impact of these radicals resulted in the production of oxygenated products
256 through oxidation reactions. In H_2 carrier gas, H radicals present in excess which can contribute
257 to the production of various hydrocarbons. The H radicals act as a scavenger for intermediate
258 to produce final products. It was noted that the selectivity to LHC was maximum in H_2 carrier
259 gas as compared to N_2 carrier gas. The methane selectivity was maximum (60%) as compared
260 to other LHC due to recombination reactions of CH_3 and H in H_2 carrier gas [49]. Similarly,
261 when H_2 was added to N_2, the selectivity to LHC significantly increases [35]. In N_2 carrier gas,
262 excited species play a major contribution towards the final products. These excited species can
263 produce benzyl and phenyl radicals which can agglomerate to produce solid residues.

264

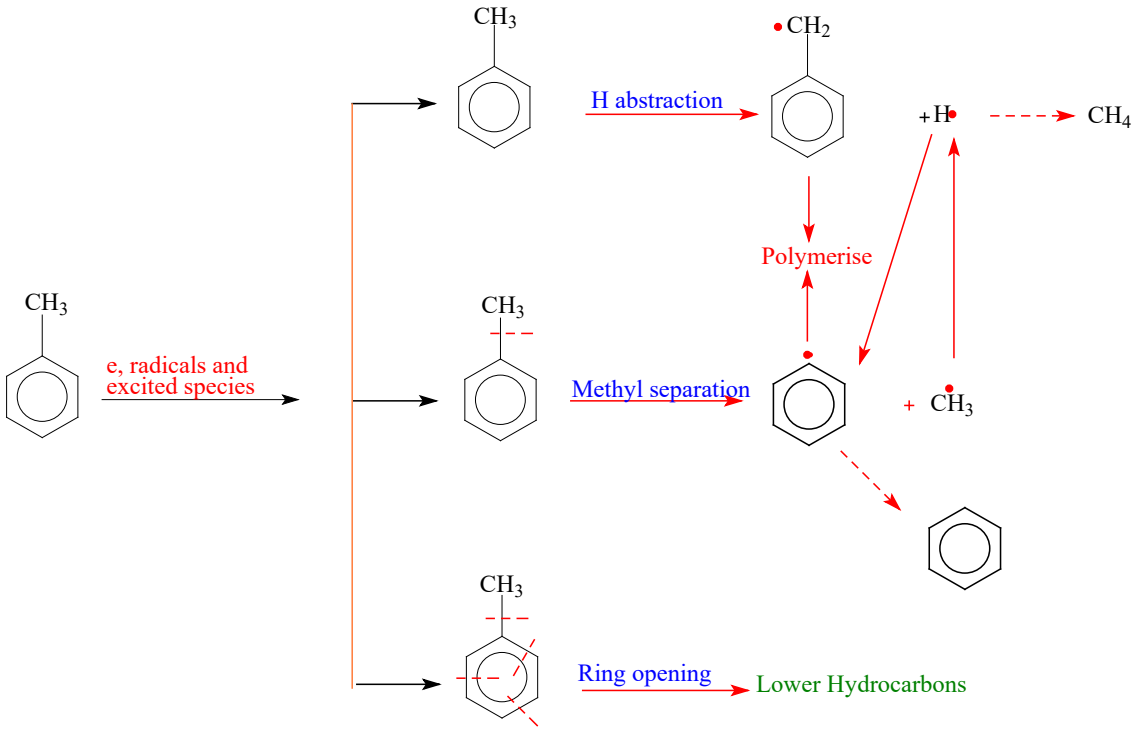

Fig.7. General Mechanism for toluene decomposition

3.7 Kinetic equation

From the literature precedence and the experimental observation in this study, a strong dependence of NTP reactions on the input energy was realized [17, 49]. Therefore, it can be concluded that the performance of the plasma reactor is greatly influenced by the input energy. Herein, the decomposition rate of toluene with respect to SIE can be written as:

$$r = -d(C_7H_8) / dSIE = k_{SIE}(C_7H_8)^n \quad (1)$$

Where the power 'n' indicates the order of the reaction and k_{SIE} is the energy constant in the given reaction. The effect of SIE on the remaining fraction of toluene using different carrier gases is shown in Fig. 8. The decomposition of toluene in CO_2, H_2, N_2 and CO reveals a similar trend having values of the R^2 in the range of 0.95–0.98. Moreover, a first-order dependence of the reaction was observed as a function of SIE in the DBD reactor for each carrier gas. Therefore, the decomposition of toluene for each carrier gas can be represented by the following equation:

$$\ln\frac{(C_7H_8)}{(C_7H_8)_0} = (-k_{SIE}\times SIE) \quad (2)$$

It was possible due to the presence of excess energetic electrons and excited species that attacked the toluene. It was reported that electron impact plays a key role in NTP reactions [56, 57]. The rates for radical reactions were very low, in the range of 10^{-22} –10^{-12}cm^3/s [58]. However, charge transfer reactions of toluene with ions and recombination of electrons and toluene's were significant (10^{-10}–10^{-7}), but densities of ions were much lower (4–5 orders of magnitude) as compared to radical densities [56, 58]. The electron density is significantly high (10^{12} cm^{-3}) in the discharge channel [59], whereas the rate of reactions is about 10^{-6} cm^3/s and a function mean energy of electrons [58]. Therefore, energetic electrons played a key role in the decomposition of toluene due to the high density and reaction rate.

From Fig. 8(a–d), it can be observed that the slope of the line was in the following order: N_2 > H_2 > CO_2 > CO, which implies that the value of energy constant follows the same order because of lower conversion of toluene.

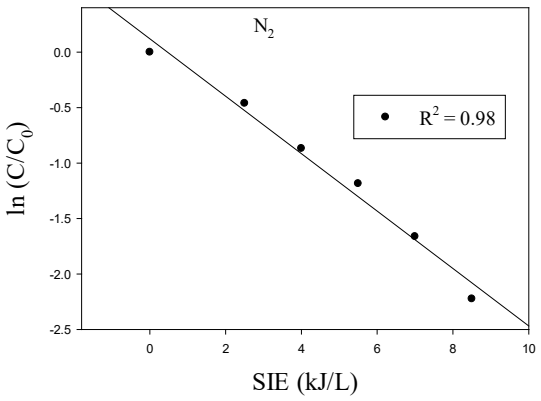

(a)

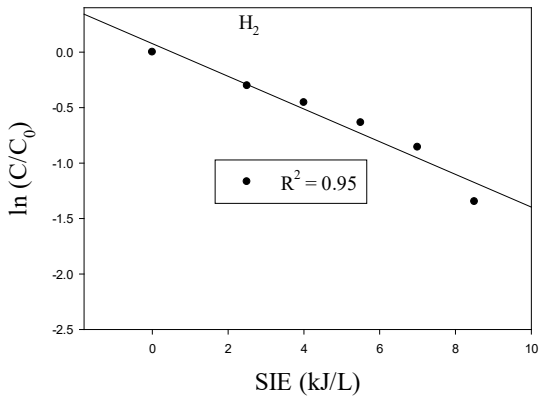

(b)

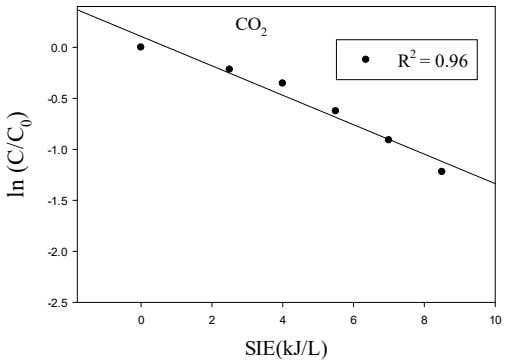

(c)

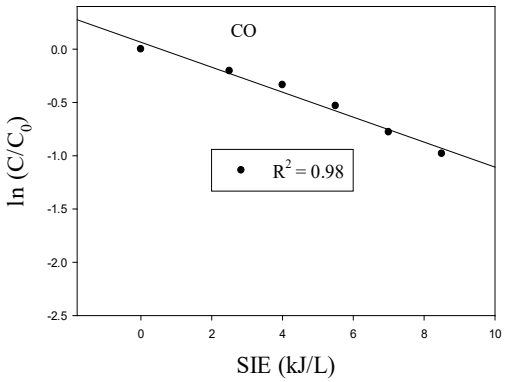

(d)

Fig. 8. Effect of SIE on the remaining fraction of toluene in different carrier gases. Reaction conditions: power, 5–17 W ;concentration, 33 g/Nm^3; flow rate, 120 ml/min; and residence time, 1.43 s. Data points of Fig. 8 (b) has been taken from our previous study for comparison [49].

4. Conclusions

It is observed that N_2 shows maximum conversion among all carrier gases, whereas CO shows a minimum. The decomposition of toluene in different carrier gases increased in the following order: CO < CO_2 < H_2 < N_2. The product distribution depends on the nature of carrier gas. Lower hydrocarbons (LHC) and solid residues formation occurred in all carrier gases. The yield of the products, i.e. CO, H_2, and LHC increased with SIE, due to the presence of more reactive species at high power. The yield of LHC was maximum in H_2 carrier gas due to the presence of H radicals, which contributed to crack the aromatic ring and produced more LHC than other carrier gases. The yield of LHC in CO_2, N_2 and CO carrier gases was less due to agglomeration reactions. The removal of toluene in all carrier gases showed first-order dependence due to the presence of energetic electrons.

References

[1] I. Narvaez, A. Orio, M.P. Aznar, J. Corella, Biomass gasification with air in an atmospheric bubbling fluidized bed. Effect of six operational variables on the quality of the produced raw gas, Industrial & Engineering Chemistry Research, 35 (1996) 2110-2120.

[2] D. Mei, S. Liu, Y. Wang, H. Yang, Z. Bo, X. Tu, Enhanced reforming of mixed biomass tar model compounds using a hybrid gliding arc plasma catalytic process, Catalysis Today, 337 (2019) 225-233.

[3] L. Devi, K.J. Ptasinski, F.J.J.G. Janssen, A review of the primary measures for tar elimination in biomass gasification processes, Biomass and bioenergy, 24 (2003) 125-140.

[4] M. Baratieri, P. Baggio, B. Bosio, M. Grigiante, G.A. Longo, The use of biomass syngas in IC engines and CCGT plants: a comparative analysis, Applied Thermal Engineering, 29 (2009) 3309-3318.

[5] U. Arena, Process and technological aspects of municipal solid waste gasification. A review, Waste management, 32 (2012) 625-639.

[6] J. Han, H. Kim, The reduction and control technology of tar during biomass gasification/pyrolysis: an overview, Renewable and sustainable energy reviews, 12 (2008) 397-416.

[7] S. Consonni, F. Viganò, Waste gasification vs. conventional waste-to-energy: a comparative evaluation of two commercial technologies, Waste management, 32 (2012) 653-666.

[8] S. Anis, Z.A. Zainal, Tar reduction in biomass producer gas via mechanical, catalytic and thermal methods: A review, Renewable and Sustainable Energy Reviews, 15 (2011) 2355-2377.

[9] P. McKendry, Energy production from biomass (part 3): gasification technologies, Bioresource technology, 83 (2002) 55-63.

[10] P.A. Simell, J.O. Hepola, A.O.I. Krause, Effects of gasification gas components on tar and ammonia decomposition over hot gas cleanup catalysts, Fuel, 76 (1997) 1117-1127.

[11] Y. Pang, H. Bosch, T. Hammer, D. Müller, J. Karl, Plasma-Aided Reforming of Toluene and Isopropanol with Analysis of Decomposition Mechanism, Waste and Biomass Valorization, 11 (2020) 675-688.

[12] F. Saleem, J. Harris, K. Zhang, A. Harvey, Non-thermal plasma as a promising route for the removal of tar from the product gas of biomass gasification – A critical review, Chemical Engineering Journal, 382 (2020) 122761.

[13] G. Petitpas, J.D. Rollier, A. Darmon, J. Gonzalez-Aguilar, R. Metkemeijer, L. Fulcheri, A comparative study of non-thermal plasma assisted reforming technologies, International Journal of Hydrogen Energy, 32 (2007) 2848-2867.

[14] K. Tao, N. Ohta, G. Liu, Y. Yoneyama, T. Wang, N. Tsubaki, Plasma enhanced catalytic reforming of biomass tar model compound to syngas, Fuel, 104 (2013) 53-57.

[15] N. Blin-Simiand, F. Jorand, L. Magne, S. Pasquiers, C. Postel, J.R. Vacher, Plasma reactivity and plasma-surface interactions during treatment of toluene by a dielectric barrier discharge, Plasma Chemistry and Plasma Processing, 28 (2008) 429-466.

[16] B. Wang, C. Chi, M. Xu, C. Wang, D. Meng, Plasma-catalytic removal of toluene over CeO 2-MnO x catalysts in an atmosphere dielectric barrier discharge, Chemical Engineering Journal, 322 (2017) 679-692.

[17] O. Karatum, M.A. Deshusses, A comparative study of dilute VOCs treatment in a non-thermal plasma reactor, Chemical Engineering Journal, 294 (2016) 308-315.

[18] H.M. Lee, M.B. Chang, Abatement of gas-phase p-xylene via dielectric barrier discharges, Plasma chemistry and plasma processing, 23 (2003) 541-558.

[19] F. Saleem, A. Harvey, K. Zhang, Low temperature conversion of toluene to methane using dielectric barrier discharge reactor, Fuel, 248 (2019) 258-261.

[20] F. Saleem, K. Zhang, A. Harvey, Direct Conversion of Benzene as a Tar Analogue to Methane Using Non-thermal Plasma, Energy & Fuels, 33 (2019) 2598-2601.

[21] A. Mahyar, H. Miessner, S. Mueller, K.H. Hama Aziz, D. Kalass, D. Moeller, K. Kretschmer, S. Robles Manuel, J. Noack, Development and Application of Different Non-thermal Plasma Reactors for the

Removal of Perfluorosurfactants in Water: A Comparative Study, Plasma Chemistry and Plasma Processing, 39 (2019) 531-544.
[22] K.H. Hama Aziz, H. Miessner, S. Mueller, D. Kalass, D. Moeller, I. Khorshid, M.A.M. Rashid, Degradation of pharmaceutical diclofenac and ibuprofen in aqueous solution, a direct comparison of ozonation, photocatalysis, and non-thermal plasma, Chemical Engineering Journal, 313 (2017) 1033-1041.
[23] K.H. Hama Aziz, H. Miessner, A. Mahyar, S. Mueller, D. Kalass, D. Moeller, K.M. Omer, Removal of dichloroacetic acid from aqueous solution using non-thermal plasma generated by dielectric barrier discharge and nano-pulse corona discharge, Separation and Purification Technology, 216 (2019) 51-57.
[24] K.H. Hama Aziz, A. Mahyar, H. Miessner, S. Mueller, D. Kalass, D. Moeller, I. Khorshid, M.A.M. Rashid, Application of a planar falling film reactor for decomposition and mineralization of methylene blue in the aqueous media via ozonation, Fenton, photocatalysis and non-thermal plasma: A comparative study, Process Safety and Environmental Protection, 113 (2018) 319-329.
[25] K.H. Hama Aziz, H. Miessner, S. Mueller, A. Mahyar, D. Kalass, D. Moeller, I. Khorshid, M.A.M. Rashid, Comparative study on 2,4-dichlorophenoxyacetic acid and 2,4-dichlorophenol removal from aqueous solutions via ozonation, photocatalysis and non-thermal plasma using a planar falling film reactor, Journal of Hazardous Materials, 343 (2018) 107-115.
[26] L. Liu, Q. Wang, S. Ahmad, X. Yang, M. Ji, Y. Sun, Steam reforming of toluene as model biomass tar to H2-rich syngas in a DBD plasma-catalytic system, Journal of the Energy Institute, 91 (2018) 927-939.
[27] U.H. Dahiru, F. Saleem, K. Zhang, A.P. Harvey, Removal of cyclohexane as a toxic pollutant from air using a non-thermal plasma: Influence of different parameters, Journal of Environmental Chemical Engineering, 9 (2021) 105023.
[28] B. Xu, J. Xie, X. Yin, H. Liu, C. Sun, C. Wu, Mechanisms of Toluene Removal in Relation to the Main Components of Biosyngas in a Catalytic Nonthermal Plasma Process, Energy & Fuels, 33 (2019) 4287-4301.
[29] M. Kong, J. Fei, S. Wang, W. Lu, X. Zheng, Influence of supports on catalytic behavior of nickel catalysts in carbon dioxide reforming of toluene as a model compound of tar from biomass gasification, Bioresource technology, 102 (2011) 2004-2008.
[30] D. Swierczynski, C. Courson, A. Kiennemann, Study of steam reforming of toluene used as model compound of tar produced by biomass gasification, Chemical Engineering and Processing: Process Intensification, 47 (2008) 508-513.
[31] F. Zhu, X. Li, H. Zhang, A. Wu, J. Yan, M. Ni, H. Zhang, A. Buekens, Destruction of toluene by rotating gliding arc discharge, Fuel, 176 (2016) 78-85.
[32] Y.N. Chun, S.C. Kim, K. Yoshikawa, Decomposition of benzene as a surrogate tar in a gliding Arc plasma, Environmental Progress & Sustainable Energy, 32 (2013) 837-845.
[33] S. Liu, D. Mei, L. Wang, X. Tu, Steam reforming of toluene as biomass tar model compound in a gliding arc discharge reactor, Chemical Engineering Journal, 307 (2017) 793-802.
[34] Y.C. Yang, Y.N. Chun, Naphthalene destruction performance from tar model compound using a gliding arc plasma reformer, Korean Journal of Chemical Engineering, 28 (2011) 539-543.
[35] F. Saleem, K. Zhang, A. Harvey, Removal of Toluene as a Tar Analogue in a N2 Carrier Gas Using a Non-thermal Plasma Dielectric Barrier Discharge Reactor, Energy & Fuels, 33 (2019) 389-396.
[36] F. Zhu, H. Zhang, H. Yang, J. Yan, X. Li, X. Tu, Plasma reforming of tar model compound in a rotating gliding arc reactor: Understanding the effects of CO2 and H2O addition, Fuel, 259 (2020) 116271.
[37] R. Xu, F. Zhu, H. Zhang, P.M. Ruya, X. Kong, L. Li, X. Li, Simultaneous Removal of Toluene, Naphthalene, and Phenol as Tar Surrogates in a Rotating Gliding Arc Discharge Reactor, Energy & Fuels, 34 (2020) 2045-2054.
[38] P. Jamróz, W. Kordylewski, M. Wnukowski, Microwave plasma application in decomposition and steam reforming of model tar compounds, Fuel Processing Technology, 169 (2018) 1-14.

[39] F. Saleem, K. Zhang, A.P. Harvey, Decomposition of benzene as a tar analogue in CO2 and H2 carrier gases, using a non-thermal plasma, Chemical Engineering Journal, 360 (2019) 714-720.
[40] X. Tu, B. Verheyde, S. Corthals, S. Paulussen, B.F. Sels, Effect of packing solid material on characteristics of helium dielectric barrier discharge at atmospheric pressure, Physics of Plasmas, 18 (2011) 080702.
[41] H. Zhang, C. Du, A. Wu, Z. Bo, J. Yan, X. Li, Rotating gliding arc assisted methane decomposition in nitrogen for hydrogen production, international journal of hydrogen energy, 39 (2014) 12620-12635.
[42] V.A. Bityurin, E.A. Filimonova, G.V. Naidis, Simulation of naphthalene conversion in biogas initiated by pulsed corona discharges, IEEE Transactions on Plasma Science, 37 (2009) 911-919.
[43] L. Yu, X. Li, X. Tu, Y. Wang, S. Lu, J. Yan, Decomposition of naphthalene by dc gliding arc gas discharge, The Journal of Physical Chemistry A, 114 (2009) 360-368.
[44] L. Yu, X. Tu, X. Li, Y. Wang, Y. Chi, J. Yan, Destruction of acenaphthene, fluorene, anthracene and pyrene by a dc gliding arc plasma reactor, Journal of Hazardous Materials, 180 (2010) 449-455.
[45] A.A. Abdelaziz, T. Seto, M. Abdel-Salam, Y. Otani, Influence of nitrogen excited species on the destruction of naphthalene in nitrogen and air using surface dielectric barrier discharge, Journal of hazardous materials, 246 (2013) 26-33.
[46] Q. Yu, M. Kong, T. Liu, J. Fei, X. Zheng, Characteristics of the decomposition of CO2 in a dielectric packed-bed plasma reactor, Plasma Chemistry and Plasma Processing, 32 (2012) 153-163.
[47] K. Zhang, G. Zhang, X. Liu, A.N. Phan, K. Luo, A Study on CO2 Decomposition to CO and O2 by the Combination of Catalysis and Dielectric-Barrier Discharges at Low Temperatures and Ambient Pressure, Industrial & Engineering Chemistry Research, 56 (2017) 3204-3216.
[48] F. Saleem, K. Zhang, A. Harvey, Role of CO2 in the Conversion of Toluene as a Tar Surrogate in a Nonthermal Plasma Dielectric Barrier Discharge Reactor, Energy & Fuels, 32 (2018) 5164-5170.
[49] F. Saleem, K. Zhang, A. Harvey, Temperature dependence of non-thermal plasma assisted hydrocracking of toluene to lower hydrocarbons in a dielectric barrier discharge reactor, Chemical Engineering Journal, 356 (2019) 1062-1069.
[50] F. Saleem, K. Zhang, A. Harvey, Plasma-assisted decomposition of a biomass gasification tar analogue into lower hydrocarbons in a synthetic product gas using a dielectric barrier discharge reactor, Fuel, 235 (2019) 1412-1419.
[51] F. Saleem, J. Umer, A. Rehman, K. Zhang, A. Harvey, Effect of Methane as an Additive in the Product Gas toward the Formation of Lower Hydrocarbons during the Decomposition of a Tar Analogue, Energy & Fuels, 34 (2020) 1744-1749.
[52] R.M. Eliott, M.F.M. Nogueira, A.S. Silva Sobrinho, B.A.P. Couto, H.S. Maciel, P.T. Lacava, Tar reforming under a microwave plasma torch, Energy & Fuels, 27 (2013) 1174-1181.
[53] J.G. Burr, R.A. Meyer, J.D. Strong, The hydrogen carrier technique for the pyrolysis of toluene, Journal of the American Chemical Society, 86 (1964) 3846-3850.
[54] F. Saleem, A.H. Khoja, J. Umer, F. Ahmad, S.Z. Abbas, K. Zhang, A. Harvey, Removal of benzene as a tar model compound from a gas mixture using non-thermal plasma dielectric barrier discharge reactor, Journal of the Energy Institute, 96 (2021) 97-105.
[55] M. Szwarc, The C–H bond energy in toluene and xylenes, The Journal of Chemical Physics, 16 (1948) 128-136.
[56] H. Kohno, A.A. Berezin, J.-S. Chang, M. Tamura, T. Yamamoto, A. Shibuya, S. Honda, Destruction of volatile organic compounds used in a semiconductor industry by a capillary tube discharge reactor, IEEE Transactions on Industry Applications, 34 (1998) 953-966.
[57] K. Urashima, J.S. Chang, T. Ito, Reduction of NO/sub x/from combustion flue gases by superimposed barrier discharge plasma reactors, IEEE Transactions on industry applications, 33 (1997) 879-886.
[58] A.W. Miziolek, J.T. Herron, W.G. Mallard, J.W. Hudgens, D.S. Green, W. Tsang, J.S. Chang, Importance of chemistry in non-thermal plasma control of volatile organic compounds and air toxics, in: Proc. ELMECO94, 1994, pp. 65-71.

[59] K. Uraahima, J.S. Chang, H. Thompson, Modeling of capillary tube plasma reactor corona discharge parameters in dry air with trace voltaile organic cornpounds [C], in: Proc 12th int symp plasma chemistry (J. Heherlein, ed.). Minneapolis, MN: Univ. of Minnesota Press, 1995, pp. 99S-1000.